

Crystallization kinetics of the bulk-glass-forming Pd₄₃Ni₁₀Cu₂₇P₂₀ melt

Jan Schroers^{a)} and William L. Johnson

California Institute of Technology, Keck Laboratory of Engineering Materials 138-78,
Pasadena, California 91125

Ralf Busch

Department of Mechanical Engineering, Oregon State University, Corvallis, Oregon 97331

(Received 31 January 2000; accepted for publication 20 June 2000)

The crystallization of undercooled Pd₄₃Ni₁₀Cu₂₇P₂₀ melts is studied under isothermal conditions and at constant heating and cooling rates. Investigations are carried out by fluxing the melt with B₂O₃ and without any fluxing material. The isothermal experiments allow us to determine the complete time–temperature–transformation diagram with a minimum crystallization time of about 200 s for the fluxed melt and about 130 s for the unfluxed Pd₄₃Ni₁₀Cu₂₇P₂₀ melt. The results of the experiments at constant cooling and heating rates are summarized in a continuous heating and cooling diagram. The critical cooling rate for the fluxed alloy is determined to be 0.09 K/s, whereas the critical heating rate is 6 K/s. For the unfluxed Pd₄₃Ni₁₀Cu₂₇P₂₀, 0.4 and 9 K/s are found, respectively. This alloy exhibits the most sluggish crystallization kinetics of all metallic systems known so far. © 2000 American Institute of Physics. [S0003-6951(00)02633-4]

Recently discovered multicomponent metallic alloys exhibit excellent glass forming ability.^{1–3} A quantitative measure for the glass forming ability is the critical cooling rate to bypass crystallization. Another quantity that determines the thermal stability of the supercooled liquid at low temperatures is the temperature difference observed during heating between the crystallization temperature T_x and the glass transition temperature T_g given by $\Delta T = T_x - T_g$. However, to obtain a more detailed description of the glass forming ability and the crystallization behavior, additional investigations have to be performed.

A characterization of the time scale for crystallization under isothermal and continuous cooling and heating conditions is given by the time–temperature–transformation (TTT) diagram together with the continuous cooling and heating (CCH) diagram. The TTT diagram represents the onset time to reach observable crystallization in an isothermal experiment as a function of temperature. Its most characteristic feature is the crystallization “nose,” where the onset time no longer decreases with decreasing temperature but increases due to the slowdown of the kinetics of the undercooled melt. The first complete TTT diagram for a metallic system was measured on Zr₄₁Ti₁₄Cu₁₂Ni₁₀Be₂₃ (Vit 1).⁴ For that alloy, the minimum crystallization time which corresponds to the nose in the TTT diagram was found to be at about 850 K and 50 s.

The cumulative time to reach crystallization in a continuous heating or cooling experiment is depicted by a continuous cooling and heating diagram. It allows us to determine the critical cooling rate R_c and critical heating rate R_h . Recently, a CCH diagram was published for Vit 1.⁵ This particular diagram revealed a large asymmetry in the crystallization behavior of amorphous samples heated from below the glass transition temperature compared to liquid samples

cooled from above the liquidus temperature. For the Pd₄₀Ni₁₀Cu₃₀P₂₀ alloy a continuous cooling diagram was reported and the influence of the B₂O₃ fluxing material was investigated.⁶ It was found earlier that fluxing the ternary PdNiP alloys with B₂O₃ enhances their glass forming ability.⁷ Recent studies on the PdNiCuP systems have shown that only a slight composition shift of the Pd₄₀Ni₁₀Cu₃₀P₂₀ alloy to Pd₄₃Ni₁₀Cu₂₇P₂₀ enlarges ΔT dramatically,⁸ suggesting that the glass forming ability of this alloy is superior to other PdNiCuP alloys.

This letter reports on crystallization studies on Pd₄₃Ni₁₀Cu₂₇P₂₀ melts that were either processed in B₂O₃ or without any fluxing material. Isothermal experiments were performed in the supercooled liquid regime. An overall TTT diagram was determined that represents the isothermal crystallization behavior without special regard to the phase formation sequence at different temperatures. Also, constant heating and cooling experiments were undertaken to determine the critical heating and cooling rate, which leads to the construction of a CCH diagram.

Amorphous samples were prepared by inductively melting the constituents in quartz tubes for 20 min at 1200 K followed by water quenching. The samples were fluxed in B₂O₃ during this procedure. Wavelength-dispersive-spectrometer measurements were carried out to verify the composition of the samples. Glassy Pd₄₃Ni₁₀Cu₂₇P₂₀ samples of about 200 mg and additional 5–10 mg B₂O₃ for the flux experiments were introduced into graphite crucibles and inductively heated in a titanium gettered argon atmosphere. The temperature was measured using a thermocouple (type K) with an absolute accuracy better than ± 2 K. In order to enhance the sensitivity of the measurement, a two-crucible setup was used similar to a standard differential thermal analyzer. A computer controlled proportional integral differential algorithm enabled isothermal anneals within ± 0.5 K of the setpoint. Details of the experimental setup can be found in Ref. 9.

^{a)}Author to whom correspondence should be addressed; Electronic mail: schroers@hyperfine.caltech.edu

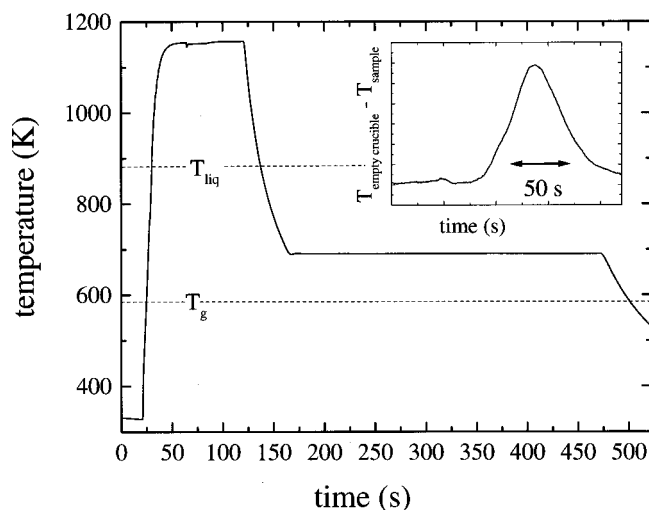


FIG. 1. Typical time-temperature profile of an isothermal experiment. Prior to the isothermal heat treatment the $\text{Pd}_{43}\text{Ni}_{10}\text{Cu}_{27}\text{P}_{20}$ sample was kept for 100 s at 1175 K. The crystallization of the melt is indicated by a temperature rise that has its origins in the release of the heat of fusion during crystallization. This is detected from the temperature difference $T_{\text{diff}} = T_{\text{empty crucible}} - T_{\text{sample}}$ as shown in the inset.

Figure 1 shows a typical temperature-time profile of an experiment performed to determine the isothermal crystallization behavior. The melt is cooled to the annealing temperature with a rate of about 10 K/s from 1175 K. The crystallization of the melt is indicated by a temperature rise that has its origin in the release of the heat of fusion during crystallization. This is detected from the temperature difference $T_{\text{diff}} = T_{\text{empty crucible}} - T_{\text{sample}}$ as shown in the inset of Fig. 1.

The results of this isothermal crystallization experiments are summarized in the TTT diagram shown in Fig. 2. In this diagram, the time at which a heat release is detected during isothermal annealing is plotted as a function of temperature. The diagram shows the typical ‘‘C’’ shape representing the crystallization without special regard to the phase formation sequence. The position of the nose, which defines the time and temperature where crystallization in this system occurs most rapidly, is at about 680 K and 200 s for the fluxed samples. For the experiments carried out without any flux the nose is at approximately 680 K and 130 s.

Heating experiments were carried out in such a way that amorphous and crystalline $\text{Pd}_{43}\text{Ni}_{10}\text{Cu}_{27}\text{P}_{20}$ samples were heated with rates between 0.2 and 6 K/s. Prior to each heating procedure, the sample was heated to 1175 K and subsequently cooled with a rate of approximately 10 K/s, which results in the formation of an amorphous sample. Crystalline samples were prepared by keeping the sample for 500 s at 675 K. The onset temperature of crystallization measured on fluxed samples upon heating with different rates are plotted in Fig. 3. With increasing heating rate the crystallization temperature measured on the fluxed samples shifts from 672 K for a rate of 0.1 K/s up to 751 K for a rate of 3 K/s. Crystallization is no longer observed during heating amorphous $\text{Pd}_{43}\text{Ni}_{10}\text{Cu}_{27}\text{P}_{20}$ with 6 K/s. In contrast, melting of crystalline $\text{Pd}_{43}\text{Ni}_{10}\text{Cu}_{27}\text{P}_{20}$ upon heating with the same rate of 6 K/s still gives a clear signal. Therefore, it can be concluded that the critical heating rate of $\text{Pd}_{43}\text{Ni}_{10}\text{Cu}_{27}\text{P}_{20}$ is approximately 6 K/s. Depending on the rate, amorphous un-

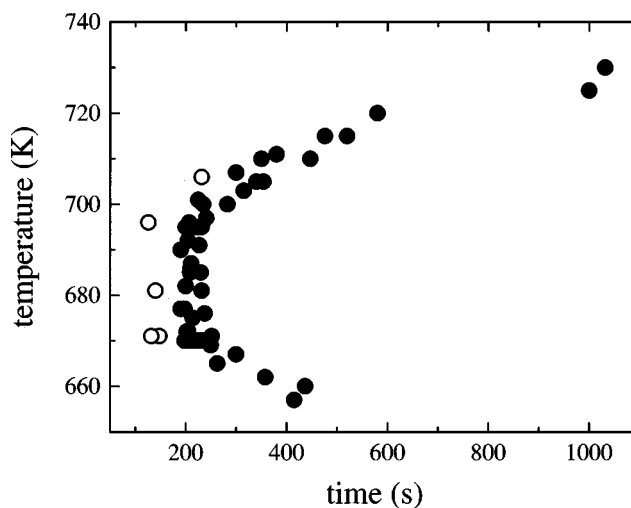


FIG. 2. Time-temperature-transformation (TTT) diagram for $\text{Pd}_{43}\text{Ni}_{10}\text{Cu}_{27}\text{P}_{20}$. In this diagram, the onset time for crystallization is shown as a function of temperature measured on fluxed (●) and unfluxed material (○).

fluxed $\text{Pd}_{43}\text{Ni}_{10}\text{Cu}_{27}\text{P}_{20}$ material crystallizes at temperatures that are up to 35 K lower than T_x measured on fluxed material. T_x increases from 673 K for a rate of 0.2 K/s up to 750 K for a heating rate of 8 K/s. The critical heating rate is determined to be about 9 K/s for the unfluxed $\text{Pd}_{43}\text{Ni}_{10}\text{Cu}_{27}\text{P}_{20}$.

In order to obtain the critical cooling rate of fluxed $\text{Pd}_{43}\text{Ni}_{10}\text{Cu}_{27}\text{P}_{20}$, the samples were cooled from 1175 K with rates between 0.05 and 0.085 K/s. T_x decreases from 702 K for a rate of 0.05 K/s to 683 K for a rate of 0.085 K/s (not shown). A rate of 0.09 K/s is sufficient to avoid crystallization upon cooling from the stable melt fluxed in B_2O_3 , whereas a rate of 0.4 K/s is measured for the unfluxed material. The critical cooling rate for fluxed $\text{Pd}_{43}\text{Ni}_{10}\text{Cu}_{27}\text{P}_{20}$ is even lower than R_c for fluxed $\text{Pd}_{40}\text{Ni}_{10}\text{Cu}_{30}\text{P}_{20}$ of about 0.3 K/s measured with the same setup.¹⁰ The results of the heating and cooling experiments are summarized in the continu-

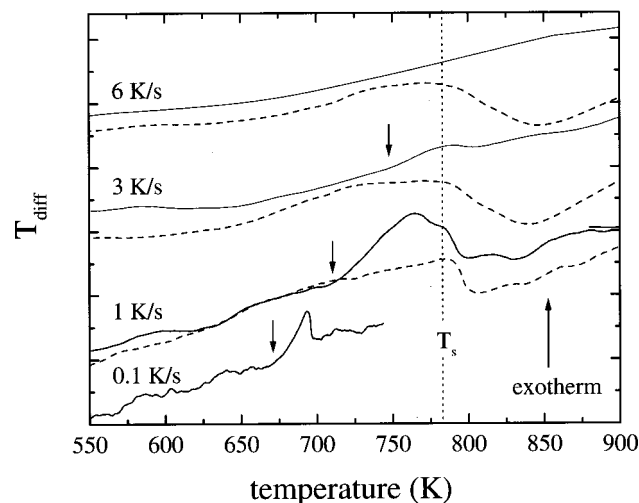


FIG. 3. Temperature difference $T_{\text{diff}} = T_{\text{empty crucible}} - T_{\text{sample}}$ as a function of temperature for amorphous (solid line) and crystalline (dashed line) $\text{Pd}_{43}\text{Ni}_{10}\text{Cu}_{27}\text{P}_{20}$ material heating with rates between 0.1 and 6 K/s. The arrows mark the onset of crystallization. The melting of the crystalline sample is indicated by an endothermic reaction beginning at the solidus temperature, $T_s = 783$ K (from Ref. 8).

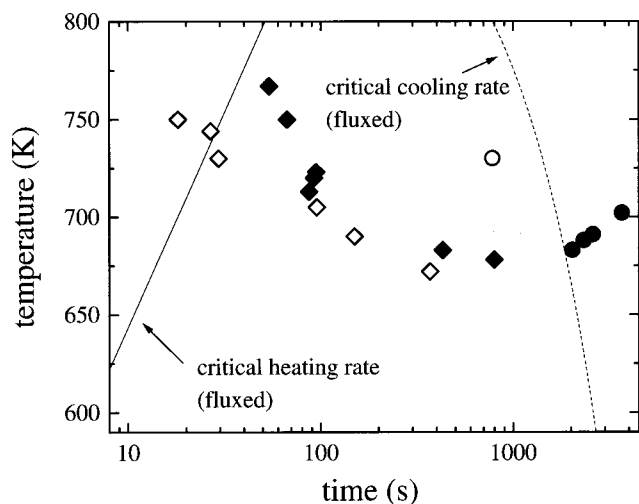


FIG. 4. Continuous cooling and heating (CCH) diagram of $\text{Pd}_{43}\text{Ni}_{10}\text{Cu}_{27}\text{P}_{20}$. In this diagram the cumulative time during constant heating and cooling from the glass transition temperature and the equilibrium liquid, respectively, is plotted vs temperature. Open circles (○) denote the onset of crystallization for unfluxed samples cooled from the equilibrium melt and solid circles (●) for the fluxed samples. The onset of crystallization for fluxed samples heated from the amorphous state is shown by solid diamonds (◆) and open diamonds (◇) denote the onset of crystallization measured on unfluxed samples. The critical cooling rate of 0.09 K/s and the critical heating rate of approximately 6 K/s for the fluxed $\text{Pd}_{43}\text{Ni}_{10}\text{Cu}_{27}\text{P}_{20}$ are denoted by the dashed and solid line, respectively.

ous heating and cooling diagram shown in Fig. 4. This diagram shows the cumulative time to reach the crystallization temperature during constant heating or cooling. It reveals a large asymmetry in the crystallization behavior upon constant heating or cooling. The critical heating rate for fluxed $\text{Pd}_{43}\text{Ni}_{10}\text{Cu}_{27}\text{P}_{20}$ of 6 K/s is one and a half orders of magnitude larger than the critical cooling rate in this system. A similar asymmetry of the crystallization behavior upon cooling and heating is also observed for the unfluxed $\text{Pd}_{43}\text{Ni}_{10}\text{Cu}_{27}\text{P}_{20}$. Kui and Turnbull¹¹ reported a critical heating rate for fluxed $\text{Pd}_{40}\text{Ni}_{40}\text{P}_{20}$ of about 3 K/s which is larger than the rate sufficient for glass formation of 1 K/s for the same fluxed material.⁷ For these heating experiments a larger scatter was reported. R_c was only sufficient for one out of five samples. A larger difference of R_c and R_h of two orders of magnitude was also reported for $\text{Zr}_{41}\text{Ti}_{14}\text{Cu}_{12}\text{Ni}_{10}\text{Be}_{23}$.⁵ In that work it was suggested that this asymmetry in the crystallization behavior upon heating or cooling is present in any metallic system. The authors attributed the asymmetry to the fact that the maximum of the nucleation rate for metallic systems is located at lower temperatures than the maximum in the growth rate, since both processes are thermally activated. The activation energy for nucleation, i.e., the energy to form a critical nucleus of some hundred atoms, is larger than the activation energy for growth, which is the activation energy for atomic diffusion. Atomic diffusion is a process where less than ten atoms are involved. The shift in temperature of the maxima of the nucleation and growth rates leads to the fact that nuclei formed during cooling at the temperature of the maximum in the nucleation rate have already passed the maximum of the growth rate. Upon heating, in contrast, the nuclei formed at the temperature of the maxi-

um of the nucleation rate are (in addition to the ones that have been formed already upon cooling) exposed to a much higher growth rate, resulting in a more rapid crystallization rate during heating.

The TTT diagram of $\text{Pd}_{43}\text{Ni}_{10}\text{Cu}_{27}\text{P}_{20}$ (see Fig. 2) suggests that most sluggish crystallization kinetics observed for a metallic system. Even in comparison to the crystallization of the very similar $\text{Pd}_{40}\text{Ni}_{10}\text{Cu}_{30}\text{P}_{20}$ alloy, investigated with the same setup,¹⁰ the crystallization of the fluxed samples takes at least 100 s more at the nose in the TTT diagram. A distinction behavior from other bulk glass forming systems such as Vit 1 is the large scatter in the onset time for crystallization in $\text{Pd}_{43}\text{Ni}_{10}\text{Cu}_{27}\text{P}_{20}$ (see Fig. 2) compared to the scatter observed in Vit 1.¹² In Vit 1, for temperatures below the nose temperature of 851 K the scattering of the onset time is less than 10% from one cycle to the other compared to 30% for $\text{Pd}_{43}\text{Ni}_{10}\text{Cu}_{27}\text{P}_{20}$. The small scattering in the onset time for Vit 1, especially at low temperatures, was explained by a diffusion-controlled process like a chemical decomposition that precedes nucleation. For PdNiCuP, in contrast, small angle neutron scattering investigations do not suggest a decomposition process prior to nucleation,¹³ which agrees with our finding that the onset times for crystallization of $\text{Pd}_{43}\text{Ni}_{10}\text{Cu}_{27}\text{P}_{20}$ are subject to relatively large statistical fluctuations. Whether the superior glass forming ability of $\text{Pd}_{43}\text{Ni}_{10}\text{Cu}_{27}\text{P}_{20}$ is due to the absence of a decomposition process or has its origin in, for example, a sluggish atomic mobility has to be addressed in future investigations.

In conclusion, the crystallization of fluxed and unfluxed $\text{Pd}_{43}\text{Ni}_{10}\text{Cu}_{27}\text{P}_{20}$ was investigated isothermally and during constant heating and cooling. The isothermal experiments resulted in the construction of the complete TTT diagram. From the continuous heating and cooling experiments the CCH diagram including the critical cooling and heating rate were derived. The results of the isothermal as well as the continuous cooling and heating experiments show that $\text{Pd}_{43}\text{Ni}_{10}\text{Cu}_{27}\text{P}_{20}$ exhibits the most sluggish crystallization behavior of all known metallic systems.

This work was supported by the National Aeronautics and Space Administration (J.S. and W.L.J.) under Grant No. NCC8-119 and the Department of Energy under Grant No. DEFG-03086ER45242 (R.B.).

¹A. Inoue, T. Zhang, and T. Masumoto, *Mater. Trans., JIM* **31**, 177 (1990).

²A. Peker and W. L. Johnson, *Appl. Phys. Lett.* **63**, 2342 (1993).

³N. Nishiyama and A. Inoue, *Mater. Trans., JIM* **37**, 1531 (1996).

⁴Y. J. Kim, R. Busch, W. L. Johnson, A. J. Rulison, and W. K. Rhim, *Appl. Phys. Lett.* **68**, 1057 (1996).

⁵J. Schroers, A. Masuhr, W. L. Johnson, and R. Busch, *Phys. Rev. B* **60**, 11855 (1999).

⁶N. Nishiyama and A. Inoue, *Acta Mater.* **47**, 1487 (1999).

⁷H. W. Kui, A. L. Greer, and D. Turnbull, *Appl. Phys. Lett.* **45**, 615 (1984).

⁸L.-R. Lu, G. Wilde, G. P. Görlner, and R. Willnecker, *J. Non-Cryst. Solids* **250–252**, 577 (1999).

⁹J. Schroers and W. L. Johnson, *Mater. Trans. JIM* (to be published).

¹⁰J. Löffler, J. Schroers, and W. L. Johnson, *Appl. Phys. Lett.* **77**, 681 (2000).

¹¹H. W. Kui and D. Turnbull, *Appl. Phys. Lett.* **47**, 796 (1985).

¹²J. Schroers, R. Busch, and W. L. Johnson, *Appl. Phys. Lett.* **76**, 2343 (2000).

¹³J. Loeffler, W. L. Johnson, W. Wagner, and P. Thiyagarajan, *Mater. Sci. Forum* (to be published).